Cold Regions Science and Technology 144 (2017) 6–15

Contents lists available at ScienceDirect

Cold Regions Science and Technology

journal homepage: www.elsevier.com/locate/coldregions

Assessing snow instability in skier-triggered snow slab avalanches by combining failure initiation and crack propagation

Johan Gaume[a,b,*], Benjamin Reuter[b]

[a] School of Architecture, Civil and Environmental Engineering, Swiss Federal Institute of Technology EPFL, Lausanne, Switzerland
[b] WSL Institute for Snow and Avalanche Research SLF, Davos, Switzerland

ARTICLE INFO

Keywords:
Snow avalanche
Skier-triggering
Failure initiation
Crack propagation
PST
Slab
Weak layer

ABSTRACT

Dry-snow slab avalanches start with a local failure in a weak snowpack layer buried below cohesive snow slab layers. If the size of the failed zone exceeds a critical size, rapid crack propagation occurs possibly followed by slab release if the slope is steep enough. The probability of skier-triggering a slab avalanche is generally characterized by classical stability indices that do not account for crack propagation. In this study, we propose a new model to evaluate the conditions for the onset of crack propagation in skier-triggered slab avalanches. For a given weak layer, the critical crack length characterizing crack propagation propensity was compared to the size of the area where the skier-induced stress exceeds the shear strength of the weak layer. The ratio between both length scales yields a stability criterion combining the processes of failure initiation and crack propagation. The critical crack length was calculated from a recently developed model based on numerical simulations. The skier-induced stress was computed from analytical solutions and finite element simulations to account for slab layering. A detailed sensitivity analysis was performed for simplified snow profiles to characterize the influence of snowpack properties and slab layering on crack propagation propensity. Finally, we applied our approach to manually observed snow profiles and compared our new criterion to Rutschblock scores.

1. Introduction

Skier-triggered slab avalanches (Fig. 1) cause more than 100 fatalities in the European Alps, each year (Techel et al., 2016). In order to improve avalanche danger forecasting and risk assessment, a sound understanding of the stability of the snowpack loaded by e.g. a skier, a snowboarder or a snowmobile is required.

A slab avalanche can be triggered, possibly remotely, by a skier if the size of the failed zone induced by the additional load of the skier in the weak layer exceeds the critical crack size (Heierli et al., 2011; Schweizer and Camponovo, 2001; Schweizer et al., 2003). If so, rapid crack propagation occurs possibly leading to a slab avalanche if the slope-parallel gravitational force overcomes friction (at a slope angle of around 30°, van Herwijnen and Heierli, 2009).

The likelihood of skier triggering has traditionally been assessed by the skier stability index (e.g., Föhn, 1987b; Jamieson and Johnston, 1998). This index is a measure to assess failure initiation by a skier. Slab layering which can affect the stress distribution in the snowpack (Schweizer, 1993) (e.g. due to the so-called bridging effect) was recently also accounted for in stability metrics (Habermann et al., 2008; Monti et al., 2016; Thumlert et al., 2013; Thumlert and Jamieson, 2014). However, this classical index, which compares weak layer strength to the sum of the shear stress due to the slab load and the additional skier stress, does not account for the second important process in snow slab avalanche release, namely crack propagation. The latter process has received much attention in the past decade (e.g. Gauthier and Jamieson, 2008; Heierli et al., 2008; van Herwijnen and Jamieson, 2007a, 2007b; Birkeland et al., 2014; Gaume et al., 2015a, 2017) and is deemed an important step after an area within the weak layer initially failed, due to an external loading. Schweizer and Camponovo (2001) evaluated the skier's zone of influence using experimental and analytical methods. This zone was defined based on pulse analysis and corresponds to the area below the skier, for a given depth, for which the stresses exceed 70% of the peak stress induced by the skier. Yet, the evaluation of this area does not involve the weak layer strength and thus does not fully characterize failure initiation.

Recently, Reuter et al. (2015) presented both a new skier stability criterion and the critical crack length required for the onset of crack propagation in the weak layer. They showed that combining these two metrics significantly improved the evaluation of snow instability. However, the skier stability index they used does not include the slab load and thus their threshold of instability may be limited to their data

* Corresponding author at: School of Architecture, Civil and Environmental Engineering, Swiss Federal Institute of Technology EPFL, Lausanne, Switzerland.
E-mail address: johan.gaume@epfl.ch (J. Gaume).

http://dx.doi.org/10.1016/j.coldregions.2017.05.011
Received 26 January 2017; Received in revised form 29 May 2017; Accepted 29 May 2017
Available online 01 June 2017

Fig. 1. Slab avalanche triggered by a snowboarder near Arlberg (Austria). Photo: Remi Petit.

set. In addition, to evaluate the critical crack length, they used the anticrack model (Heierli et al., 2008) which was recently shown to significantly overestimate the critical length on steep slopes, which is where avalanches actually release (Gaume et al., 2017).

To improve previous methods, we propose a mechanical criterion for snow instability which combines failure initiation and crack propagation in a weak snow layer below a cohesive snow slab in presence of an additional line load corresponding to a skier. This criterion compares the length of the area where the stresses induced by the slab and the skier exceed the weak layer strength to the critical crack length a_c for crack propagation.

The recent model of Gaume et al. (2017) based on discrete element simulations (Gaume et al., 2015a) is used to compute the critical crack length a_c. The stress field along the weak layer is computed from analytical solutions (Monti et al., 2016) and finite element simulations to account for slab layering (Habermann et al., 2008; Reuter et al., 2015). By comparing the stress to the weak layer strength, one can thus determine the length l_{sk} of the area where the stress exceeds the strength and compare it to a_c. A sensitivity analysis is performed for simplified snow profiles to characterize the influence of snowpack properties and slab layering on the skier crack propagation propensity. Finally, we applied our approach to a field dataset consisting of 160 Rutschblock test results with corresponding snowpit data including snow density and shear frame measurements.

2. Methods

2.1. Instability criterion

We consider a two-dimensional slab-weak layer system. The slab is characterized by its thickness D, density ρ, elastic modulus E, and Poisson's ratio ν. The weak layer is characterized by its shear strength τ_p, its shear modulus G_{wl} and thickness D_{wl}. The slope angle is denoted by ψ. The onset of crack propagation occurs if the skier crack length

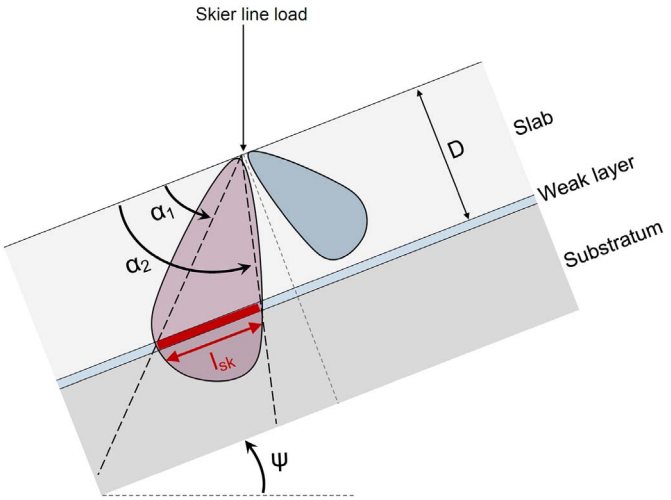

Fig. 2. Schematic of the shear stresses in the snowpack under the influence of a skier line load. The red and blue bulbs illustrate the contour of the shear stress in the snowpack. For the red bulb (left), the shear stress is equal to the shear strength of the weak layer. (For interpretation of the references to colour in this figure legend, the reader is referred to the web version of this article.)

exceeds the critical crack length i.e. if $l_{sk} > a_c$.

2.1.1. Failure initiation: skier crack length l_{sk}

The skier crack length is obtained by solving:

$$\tau + \Delta\tau > \tau_p \tag{1}$$

where $\tau = \rho g D \sin\psi$ is the shear stress due to the slab weight, $\Delta\tau$ is the additional shear stress due to the skier line load R which is defined as (Föhn, 1987b; Monti et al., 2016):

$$\Delta\tau = \frac{2R\cos\alpha \sin^2\alpha \sin(\alpha + \psi)}{\pi D} \tag{2}$$

where α is the angle between the snow surface and the line from the skier to the point of interest in the weak layer. For the case that the strength of the weak layer τ_p is exceeded along a length l_{sk} within the weak layer, we define two angles α_1 and α_2, locating the edges of this band (of failure). Hence, solving Eq. (1) corresponds to finding the two angles α_1 and α_2 where $\tau + \Delta\tau = \tau_p$ (Fig. 2). Based on geometry relations, the skier crack length l_{sk} can be evaluated by:

$$l_{sk} = D\left[\frac{1}{\tan\alpha_1} - \frac{1}{\tan\alpha_2}\right]. \tag{3}$$

Eq. (1) cannot be solved analytically for $\psi \neq 0$, i.e. if $\tau \neq 0$. It was thus solved using Matlab (fzero function). If the strength of the weak layer τ_p is not exceeded, the skier crack length l_{sk} is zero.

2.1.2. Crack propagation: critical crack length a_c

As a measure for crack propagation propensity, we compute the critical crack length a_c using the new formulation proposed by Gaume et al. (2017):

$$a_c = \Lambda\left[\frac{-\tau + \sqrt{\tau^2 + 2\sigma(\tau_p - \tau)}}{\sigma}\right] \tag{4}$$

wherein $\sigma = \rho g D \cos\psi$ and Λ is a characteristic length of the system associated with the elastic mismatch between the slab and the weak layer. It is given by:

$$\Lambda = \sqrt{\frac{E' D D_{wl}}{G_{wl}}} \tag{5}$$

with $E' = E/(1-\nu^2)$.

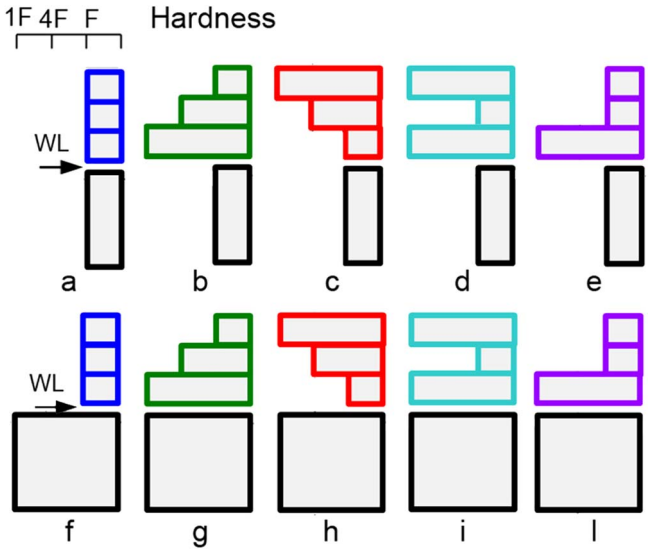

Fig. 3. Ten simplified hardness profiles. The profiles from (a) to (e) have a weak base, while from (f) to (l) a strong base. The arrows highlight the depth where the weak layer was located (not to scale). The simplified profiles have the same characteristics as the ones used by Habermann et al. (2008).

2.2. New stability index

In order to combine the metrics of failure initiation and crack propagation, we follow the concept of the stability index but use a ratio of length scales, which gives in our case:

$$S_p = \frac{a_c}{l_{sk}} \tag{6}$$

Large values of the skier crack length l_{sk} and/or low values of the critical crack length a_c lead to low stability and vice versa.

2.3. Simplified snow profiles and finite element simulations

We calculated the skier crack length for five different typical slab profiles with either a hard or soft basal layer (Fig. 3) using the finite element method (FEM), which allows to take into account snowpack layering. The FE model is described in detail in Reuter et al. (2015). The domain is divided into 2-D, quadrilateral plane strain elements with eight nodes each. The mesh was fine enough to avoid mesh size effects. The model was implemented in ANSYS workbench to calculate the skier stress within the weak layer. Linear elastic material behavior was assumed. The skier load was modeled as a static line load $R = 780$ N (Schweizer and Camponovo, 2001).

The simplified profiles have the same characteristics and material properties (Table 1) as those used by Habermann et al. (2008). The values of hand hardness (Fierz et al., 2009) were assigned corresponding to the layer densities (Geldsetzer and Jamieson, 2001). The Poisson's ratio was assumed constant $\nu = 0.2$. The slab layers have a thickness of 0.12 m each, the weak layer of 0.05 m and the basal layer of 0.8 m, thick enough to ensure that the results are not influenced by the thickness of the basal layer. As in Habermann et al. (2008) and Monti et al. (2016), the penetration depth of the skier was not taken into account for these calculations. The weak layer shear strength τ_p was assumed equal to 600 Pa and the slope angle ψ was taken equal to 38°.

Table 1
Material properties of the layers for the simplified snow profiles.

Layer characteristic	Hand hardness index	Density ρ (kgm^{-3})	Elastic modulus E (MPa)	Poisson's ratio ν
Soft	F	120	0.3	0.2
Medium	4F	180	1.5	0.2
Hard	1F	270	7.5	0.2
Weak layer	F-	100	0.15	0.2

The critical crack length was evaluated for each profile using Eqs. (4) and (5). For the elastic modulus of the slab, we used the bulk modulus computed using FEM simulations (Reuter et al., 2015), as it accounts for slab layering.

2.4. Field data

The skier crack length l_{sk} and critical crack length a_c were calculated for 160 manually observed snow profiles collected in the Columbia Mountains of Western Canada by researchers from the University of Calgary, each including at least one Rutschblock (RB) test (Föhn, 1987a). This dataset was already used in Monti et al. (2016) to validate a simplified approach to evaluate the skier-induced stress in a multi-layered snowpack. The manual snow profile observations include multiple density measurements of slab and weak layers as well as shear frame measurements of the weak layer shear strength (Jamieson and Johnston, 2001) and the penetration depth PS which was accounted for in this analysis (Reuter et al., 2015). The elastic modulus of the weak layer and of the different layers of the slab were derived from manual density measurements using the relation proposed by Scapozza (2004). All layers were implemented in the FEM model to compute the skier crack length and the bulk modulus was used to compute the critical crack length.

The values of a_c and l_{sk} were then compared to the RB score for 3 different cases corresponding to different values of the skier line load R according to Schweizer and Camponovo (2001): (i) skier standing i.e. $R = 780$ N; (ii) skier weighting i.e. $R = 1950$ N; (iii) skier jumping i.e. $R = 3900$ N (for a constant penetration depth PS as recorded for each profile).

3. Results

3.1. Sensitivity analysis

We performed a sensitivity analysis to assess the effect of snowpack properties on the skier crack length l_{sk}, the critical crack length a_c and propagation stability index S_p. First, only one parameter was varied while keeping all others unchanged. Second, to mimic more realistic snow properties, we used empirical formulations to relate (i) slab density to slab thickness, (ii) slab elastic modulus to slab density and (iii) weak layer shear strength to the overlying slab load.

3.1.1. Independent snowpack properties

Fig. 4 shows the results of the sensitivity analysis with independent snowpack properties with a weak layer shear strength of 700 Pa. As shown in Gaume et al. (2017), the critical crack length a_c decreases with increasing slab thickness D, slope angle ψ and slab density ρ, but increases with increasing elastic modulus of the slab E. On the other hand, the skier crack length l_{sk} increases with increasing slab thickness, slope angle and slab density, since the slope-parallel load increases. However, the skier crack length does not change with increasing elastic modulus because stresses are independent of the modulus, as long as the slab is uniform (Eq. 1). As a result of these trends, the propagation stability index S_p decreases with increasing slab thickness, slope angle and slab density but increases with increasing elastic modulus.

From Fig. 4, one can distinguish four different stability regimes: (i) a regime in which neither failure initiation nor crack propagation are possible because $l_{sk} = 0 < a_c$. In this case $S_p \rightarrow \infty$; (ii) a regime in which failure initiation is possible but crack propagation cannot occur since $l_{sk} < a_c$, i.e. $S_p > 1$; (iii) a regime in which both failure initiation and crack propagation occur since $l_{sk} > a_c$, i.e. $S_p < 1$ and finally (iv) a

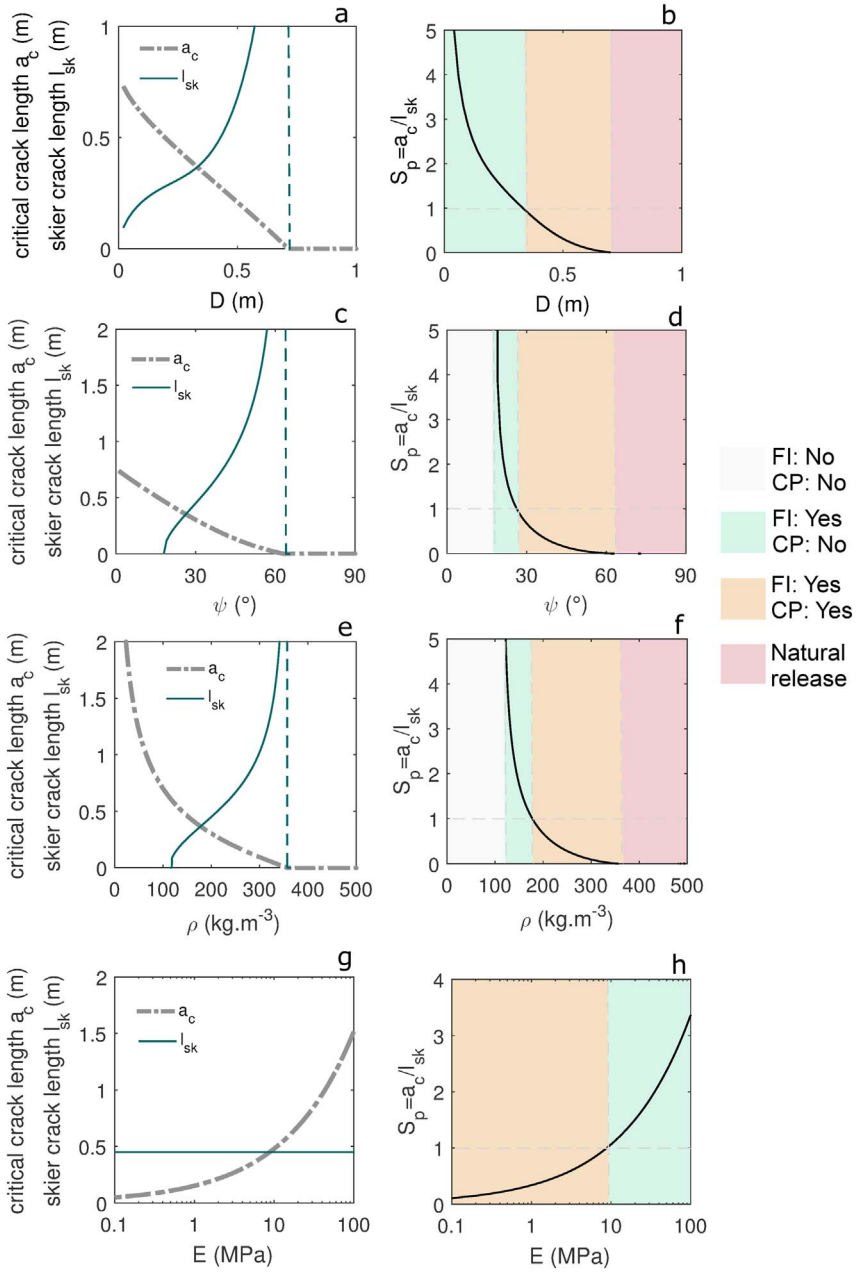

Fig. 4. Sensitivity analysis with independent snowpack properties, i.e. only one parameter was varied while the other properties were kept constant. D = 0.4 m, $\psi = 30^{\circ}$, ρ = 200 kg m^{-3}, τ_p = 700 Pa, E = 4 MPa, R = 780 N. FI: Failure initiation; CP: Crack propagation. Left column: skier crack length and critical crack length; right column: skier propagation index.

regime that is a priori unstable since the stress due to the load of the slab at the depth of the weak layer is higher than its strength. In this case, the critical crack length is equal to zero and the skier crack length is infinite leading to $S_p = 0$.

3.1.2. *Effect of slope angle: shear vs compressive failure*

In the previous section, the shear strength of the weak layer was fixed to 700 Pa for the sake of simplicity. However, it was shown that the shear strength of weak snow layers strongly depends on slope angle and that snow can also fail under compression (Chandel et al., 2014; Reiweger et al., 2015). Yet, the shear strength is significantly smaller than the compressive strength. If we use the failure envelope described in Reiweger et al. (2015) for typical snowpack values used in Fig. 4, the shear strength τ_p decreases with increasing slope angle to values between 500 and 200 Pa, while the total shear stress $\tau + \Delta\tau$ is larger than 500 Pa (Fig. 5a). On the other hand, the compressive strength σ_p is approximately constant equal to 2500 Pa (for fast loading) while the total compressive stress is < 1700 Pa (Fig. 5b). Hence, as suggested by Schweizer et al. (2016a), failure initiation is more likely to occur in shear rather than compression. This is true even on flat terrain, mostly because snow is weaker in shear than in compression, but also because skier-induced shear and compressive stresses are of the same order of magnitude as shown in Fig. 5a and b. This outcome is also illustrated by Fig. 6 which shows the shear stress profile below a skier on the flat obtained through FE simulations for typical snowpack properties. Fig. 5c and d show that both failure initiation and crack propagation can occur at slope angles larger than 10° – possibly resulting in remote avalanche triggering in adequate adjacent terrain.

3.1.3. *Realistic snowpack properties*

The elastic modulus of snow is in first order related to snow density (e.g., Camponovo and Schweizer, 2001; Scapozza, 2004; van Herwijnen

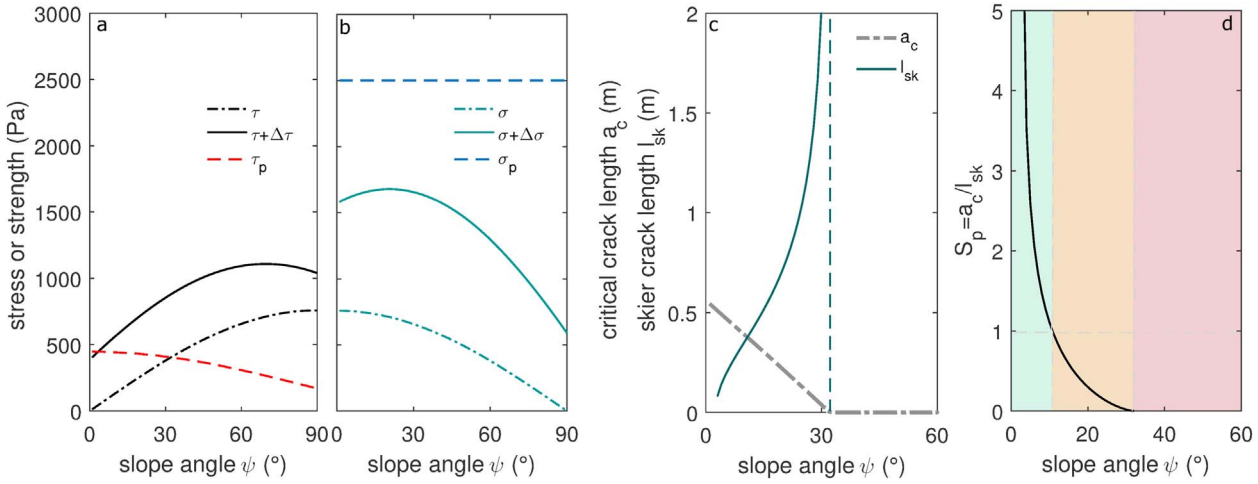

Fig. 5. Effect of slope angle on the shear (a) and compressive (b) stresses, total stresses and strengths. Effect of slope angle on (c) the critical crack length, skier crack length and (d) propagation index obtained with the Mohr-Coulomb-Cap failure envelope of Reiweger et al. (2015). D = 0.4 m, ρ = 200 kg m^{-3}, E = 4 MPa, R = 780 N.

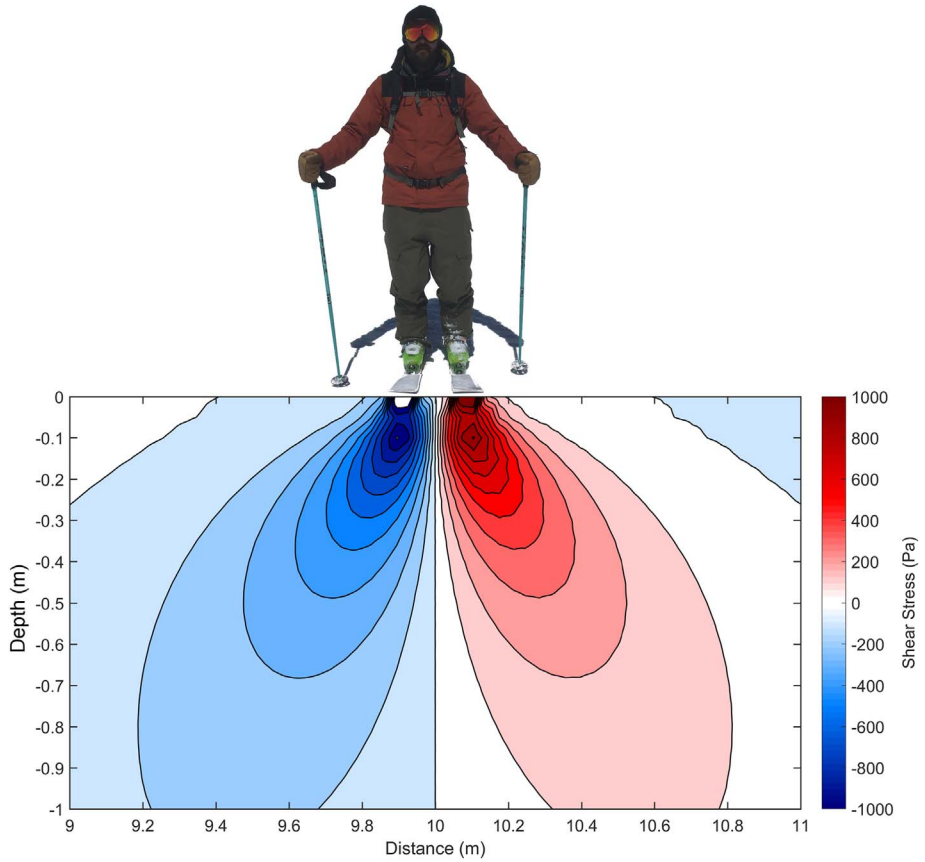

Fig. 6. Shear stress distribution on the flat in a uniform snowpack computed with finite element simulations for ρ = 200 kg m^{-3}, E = 4 MPa, R = 780 N.

et al., 2016). In general, the slab density increases with increasing thickness due to settlement processes thus affecting the elastic modulus but also inducing a strengthening of the buried layers. We assume slab density to be related to slab thickness according to $\rho = 100 + 135\,D^{0.4}$ (McClung, 2009) (with an initial density of 100 kg m^{-3} for $D = 0$, D in meters) and the shear strength to be related to slab thickness according to $\tau_p = 300 + 1370\,D^{1.3}$ (D in meters). The latter is the same expression as found by Bazant et al. (2003) and McClung (2003) with a cohesion c = 300 Pa. Finally, we assume the elastic modulus of the slab to be related to density according to a power law fit to the data of Scapozza (2004): $E = 5.07 \times 10^9(\rho/\rho_{ice})^{5.13}$ with ρ_{ice} = 917 kg m^{-3}.

Using these relationships, the stability behavior is significantly different (Fig. 7a) from the sensitivity analysis with independently varying properties. In this case, the critical crack length remains almost independent of slab thickness. The reason is that, as the elastic modulus of the slab and the strength of the weak layer increase, they counterbalance the increase of load. Furthermore, the skier crack length first increases strongly up to about D ≈ 0.3 m and then decreases. The skier crack length is higher than the critical crack length for thin snowpacks (0.1 m < D < 0.55 m) and lower for thicker ones (D > 0.55 m). As a consequence, the propagation stability index is lower than 1 for D < 0.55 m and crack propagation is possible. For slabs thicker than

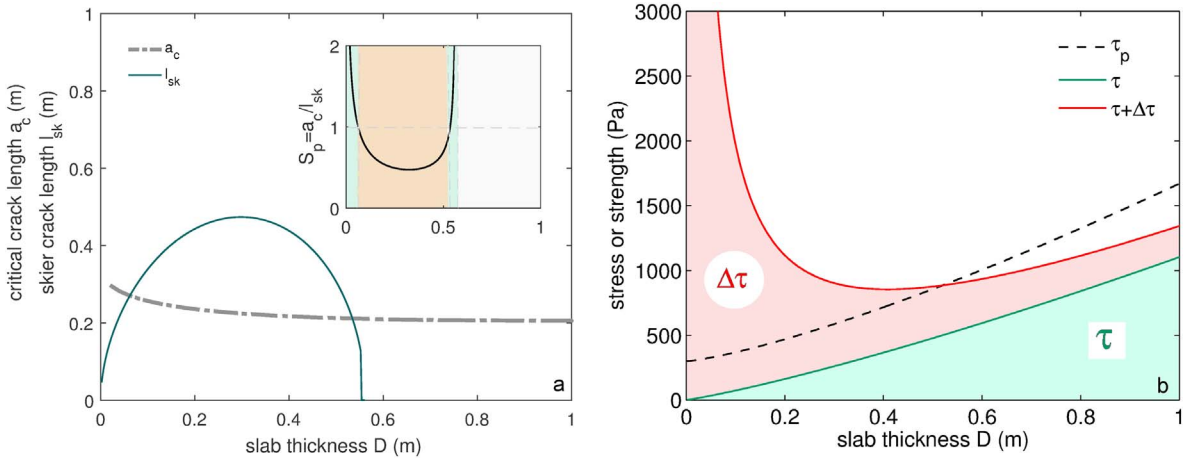

Fig. 7. Sensitivity analysis for realistic snowpack properties for $\psi = 30^{\circ}$, i.e. weak layer shear strength, slab thickness and slab density are interrelated. (a) skier and critical crack lengths vs slab thickness; (b) Shear stress τ due to the slab (green area), total stress as the sum of the shear stress due to the slab and skier additional shear stress $\Delta\tau$ (red area) and shear strength (dashed line) vs slab thickness D. (For interpretation of the references to colour in this figure legend, the reader is referred to the web version of this article.)

0.55 m, the skier-induced stress is too low; skier-triggering is not possible. This is also seen in Fig. 7b which shows the influence of slab thickness on the components of the total stress highlighting the key role of the skier-induced stress. Due to the sharp decrease of the skier-induced stress with depth, the total stress does not reach the weak layer strength for weak layers deeper than 0.55 m. This result is in line with previous field observations and measurements (e.g., Schweizer and Jamieson, 2001; van Herwijnen and Jamieson, 2007a). Note, however, that very shallow slabs are often associated with very low slab densities (excluding wind slabs) for which slab fractures might occur before the onset of crack propagation (Gaume et al., 2015b; Schweizer et al., 2014; Reuter et al., 2016a).

3.2. Influence of slab layering

The influence of slab layering was studied with FEM purely elastic simulations of simplified profiles. The total shear stress $\tau + \Delta\tau$ computed for each profile is shown in Fig. 8a and b. We chose a shear strength of 600 Pa in order to have a non-zero skier crack length which led in this particular case to stability values below 1 for most profiles. In general, profiles with a hard basal layer led to higher additional stresses at the depth of the weak layer. Hence, for a given weak layer shear strength with a hard basal layer longer skier crack lengths were observed (inserts in Fig. 8a and b). This result is apparent also in Fig. 8c where profile types were ranked by their modeled propagation stability index. Compared to their corresponding profile type with a soft basal layer, the profile types with a hard basal layer had a higher skier crack length, and thus a lower propagation stability index. This is in line with empirical results presented by van Herwijnen and Jamieson (2007a), who observed an increase in the probability of skier-triggering for harder basal layers and with results from finite element simulations of Habermann et al. (2008). Furthermore, profile types with a hard layer close to the weak layer showed a lower propensity for initiation and propagation (higher S_p) compared to those with a hard layer close to the snow surface (i.e. the red profile types in Fig. 8c). Note, however, that for this theoretical analysis the skier penetration depth was not accounted for.

3.3. Comparison with field data

We compare our skier crack length and critical crack length to field data of Rutschblock tests, i.e. the RB score. The RB scores were correlated with the critical crack length (Fig. 9c, Pearson's correlation coefficient and p-value: $r = 0.50, p < 0.001$). The critical crack length increased from approximately 0.5 m to 1.2 m for RB scores increasing from 1 to 7. The skier crack length was computed for different cases: (i) skier standing i.e. $R = 780$ N; (ii) skier weighting i.e. $R = 1950$ N; (ii) skier jumping i.e. $R = 3900$ N. A correlation analysis revealed that the skier crack length computed for the case of a skier jumping reproduced best the observed stability (RB score). Indeed, for most observed snowpack layerings, the skier crack length was zero when using the additional load corresponding to a skier standing. Hence, $R = 3900$ N - corresponding to a skier jumping - was used to compare the skier crack length to Rutschblock data. Fig. 9a shows that the skier crack length decreased overall from 0.5 m to zero for RB scores increasing from 1 to 7. The RB score was also correlated with the skier crack length ($r = -0.26$, $p < 0.001$), although the correlation was weaker than with the critical crack length. For the case RB = 1, the skier crack length and critical crack length do not fit the trend mostly because this RB class contains only 5 data points. The scatter plot in Fig. 9b shows that the skier crack length decreases with increasing critical crack length and the two quantities are correlated ($r = -0.33$, $p < 0.001$). Still, the simple criterion $l_{sk} > a_c$ i.e. $S_p < 1$ does not exclude all data points with low RB scores (RB < 3). In fact, for the presented data set a criterion $l_{sk} > a_c/3$ i.e. $S_p < 3$ would perform better, as indicated by the dashed line in Fig. 9b. Finally, we checked whether both the skier crack length and critical crack length discriminated between three stability classes defined according to the RB score: “poor” corresponding to RB = [1 2 3], “fair” to RB = [4 5] and good to RB = [6 7], the Mann-Whitney U test confirmed good discrimination of both parameters ($p < 0.05$) for all stability class combinations (poor to fair; fair to good; poor to good).

4. Discussion

Our new model allows snow instability to be described by a combination of failure initiation (skier crack length) and crack propagation (critical crack length). We compared the crack length due to a skier, i.e. the length at the depth of the weak layer for which the shear stress due to the slab and the skier exceeds the shear strength of the weak layer, to the critical crack length. The critical crack length was computed from a recent model based on discrete element simulations (Gaume et al., 2017). A detailed sensitivity analysis was performed to study the effect of snowpack properties. In particular, the effect of slope angle was assessed by using the failure envelope of typical weak snow layers based on laboratory experiments (Reiweger et al., 2015). Apparently, even on flat terrain, failure initiation is more likely in shear than in compression and the onset of crack propagation can occur on gentle slopes – as often observed by a “whumpf” sound. Using realistic relations between the snowpack properties according to empirical data, we found that the

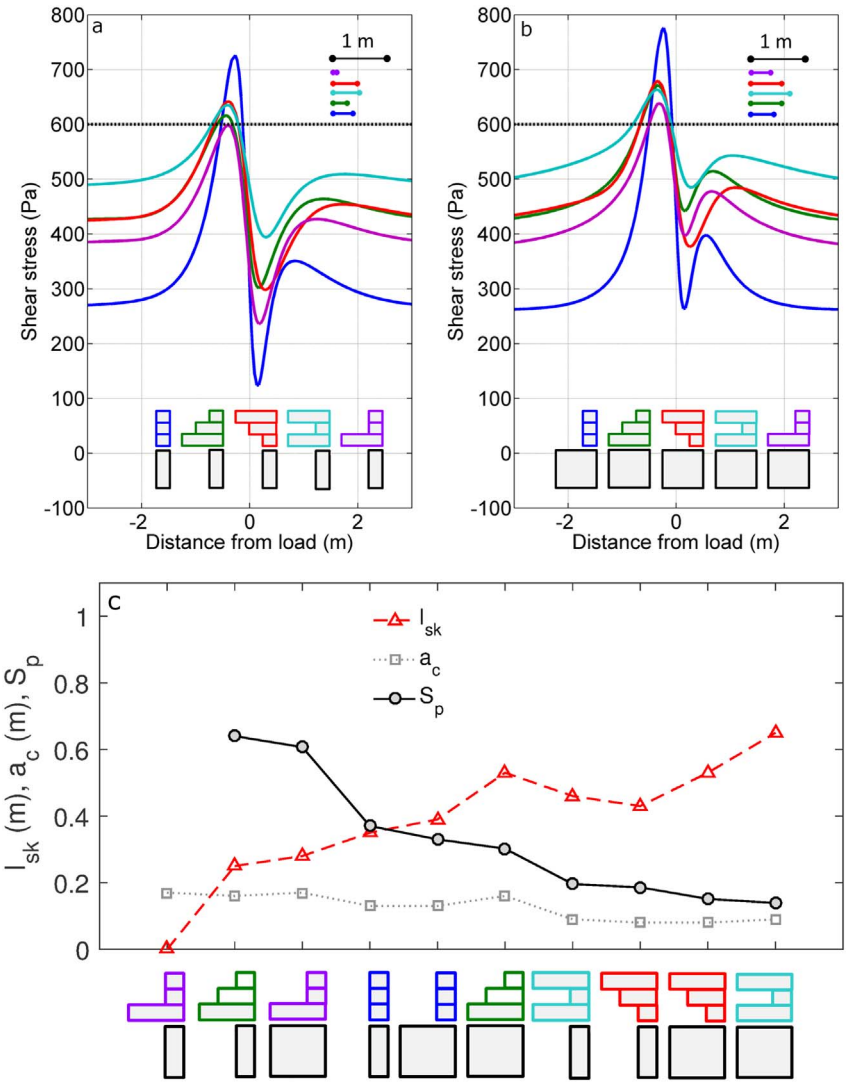

Fig. 8. Shear stress at the depth of the weak layer as a function of the distance from the skier loading for simplified snow profiles with (a) a soft basal layer and (b) a hard basal layer; inserts illustrating skier crack length for a weak layer shear strength of 600 Pa. (c) Skier crack length, critical crack length and skier propagation index as a function of the profile type sorted to obtain a decreasing trend of S_p. For the three graphs the slope angle is equal to 38°.

skier failure initiation propensity first increased with increasing slab thickness and then decreased for a thickness of about 0.6 m. This threshold depends on the chosen snowpack properties; in particular, it should increase with increasing slope angle, since a_c decreases and l_{sk} increases with increasing ψ. Failure initiation due to skier loading frequently occurs in weak layers buried about 0.5 m, and becomes infrequent for slabs thicker than about 1 m deep (van Herwijnen and Jamieson, 2007a). In particular, our model allows to refine the schematic representation of the influence of weak layer depth on failure initiation and crack propagation proposed by van Herwijnen and Jamieson (2007a). While the critical crack length is almost unaffected by weak layer depth, the skier crack length sharply decreases for deeply buried weak layers, thus reducing the probability of skier-triggered avalanches (Fig. 7). Hence, whereas on skis failure initiation may be unlikely in a weak layer buried deeper than 1 m, the critical stress may be still reached by a person without skis as this would increase the penetration depth and decrease the loading surface.

The skier crack length we proposed as a measure of failure initiation propensity is different from the skier's zone of influence described in Schweizer and Camponovo (2001). In the latter study, the zone of influence corresponds to the area where the stress distribution is affected by the presence of the skier, but no information whether the stress actually overcomes the weak layer strength is included. This is why Schweizer and Camponovo (2001) observed a monotonic increase in the skier's zone of influence with increasing depth (with a decreasing amount of stress), whereas after a certain depth (which depends on snowpack properties) our skier crack length sharply decreased with increasing depth (Fig. 7). We assume that the skier's zone of influence measured and modeled in Schweizer and Camponovo (2001) would be rather related to our model parameter Λ. The latter characterizes the length over which the stress distribution would be influenced by a (hypothetical) crack in the weak layer (Gaume et al., 2013). For typical snowpack properties, this length is between 0.2 and 0.4 m which is in agreement with the skier's length and width of influence found in Schweizer and Camponovo (2001) which varied between 0.15 and 0.6 m (half length). These typical values should also explain why they found no significant cumulative effects at a depth of ~0.25 m, when two skiers were walking one behind the other. Indeed, at this depth and for the density they measured, Λ would not be larger than 0.2 m and Gaume et al. (2013) showed that cumulative effects would occur only if the distance between two skiers (or two cracks in the weak layer) is lower than approx. 4Λ (~0.8 m), which is lower than the distance between two pairs of skis. Cumulative effects may occur for harder snowpacks since Λ increases with snow hardness ($\Lambda \sim \sqrt{E}$).

The effect of snowpack layering on the skier crack length, critical crack length and skier propagation index was quantified by means of

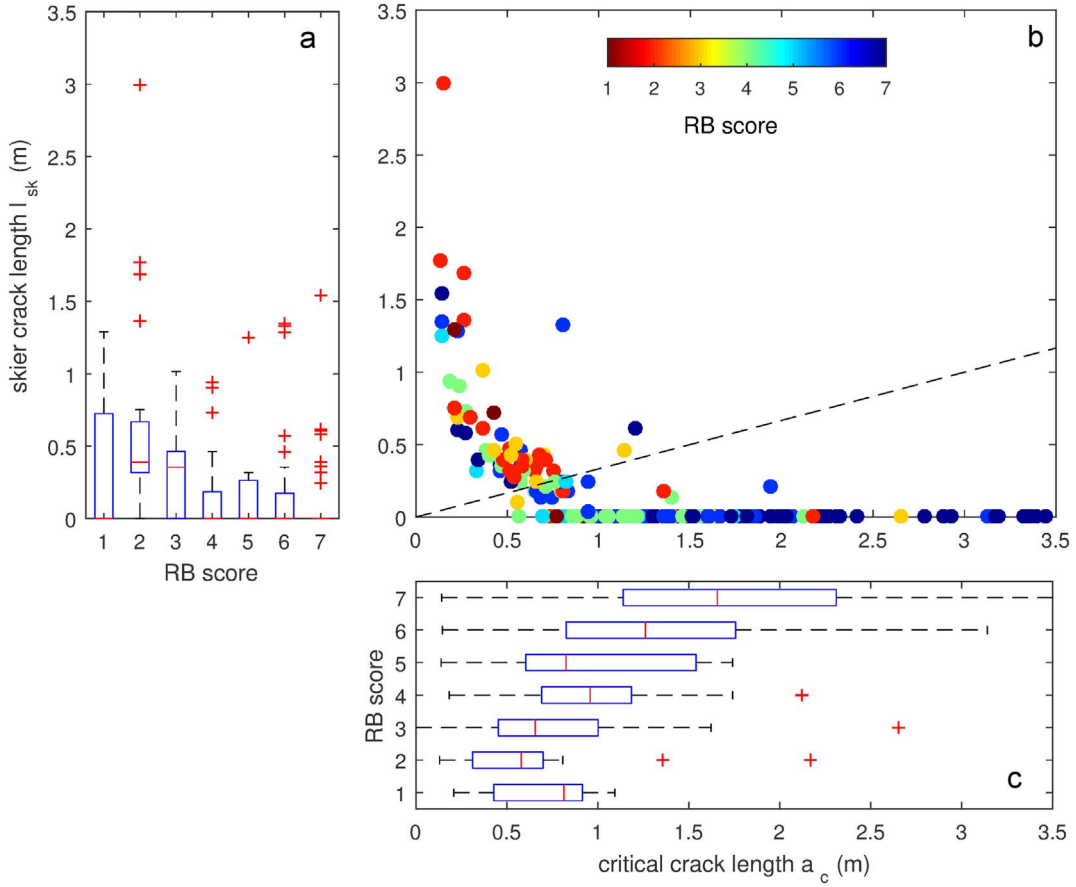

Fig. 9. (a) Skier crack length vs RB score (assuming a skier load of $R = 3900$ N). (b) Skier crack length vs critical crack length. The colors represent the RB score and the two dashed lines represent $a_c = 0.75$ m and $l_{sk} = 0.25$ m. (c) RB score vs critical crack length.

finite element simulations with a linear-elastic assumption. We confirmed that snowpacks with hard basal layers result in lower values of the skier propagation index compared to softer basal layers. This reduction in stability is due to higher stresses at the depth of the weak layer and is in line with the experimental results of van Herwijnen and Jamieson (2007a) who observed an increase in skier triggering with increasing hardness difference between the weak layer and the layer below. In addition, it was shown that snow slabs with increasing hardness with increasing depth were less prone to failure initiation and crack propagation than snowpacks that transitioned from hard to soft with a soft layer adjacent to the weak layer. Note however that skier penetration depth was not considered for the sake of simplicity of this analysis, but will likely influence the presented results, in particular those with a soft slab layer near the surface. Concerning the different simplified profiles we simulated, the density and the elastic modulus were interrelated leading to different loads on the weak layer. Additional FE simulations (not shown) were performed with uniform slab density resulting in a constant load on the weak layer, and again assuming the same shear strength for all profiles. These simulations confirmed that stiff slab layers led to lower stresses at the depth of the weak layer resulting in lower skier crack lengths compared to the cases with less stiff slab layers. Also, for the sake of simplicity, we kept the shear strength constant in our simulations of simplified profiles, whereas in reality the shear strength would increase with increasing load due to settlement and sintering (cf Section 3.1.3) (e.g. Jamieson and Schweizer, 2000; Schweizer et al., 2016b). In general, the shear strength of the weak layer adapts to the static load. This is why Reuter et al. (2015) did not consider the static stress in their stability formulation but only the dynamic part of the load induced by a skier, in contrast to our approach. As snow is known to be highly strain-rate dependent (Schweizer et al., 2003; Reiweger et al., 2015), future work will be required to assess the validity of these different assumptions.

The so-called bridging effect which causes stresses to spread out laterally and hence decreases the depth to which a given level of stress penetrates (Schweizer and Jamieson, 2003; Thumlert and Jamieson, 2014) was not accounted for in the first analytical model proposed by Föhn (1987b) based on Boussinesq's theory, which we used in the sensitivity analysis. This is exemplified by Fig. 4g where the skier crack length is independent on the slab elastic modulus. Recently, Monti et al. (2016) proposed a method to correct slab thickness D in the expression of $\Delta\tau$ for a snowpack with layers of different elastic moduli. The equivalent slab thickness $D_e = D\sqrt[3]{E/E_{wl}}$ is related to the ratio between the elastic modulus of the slab and the elastic modulus of the weak layer. Hence, if the slab is harder than the weak layer, the equivalent thickness D_e is larger than D, leading to a decrease in $\Delta\tau$. The bridging effect is naturally accounted for in our FE analysis and consequently included in our analysis of field data. The effect leads to a decrease of the skier crack length l_{sk} with increasing slab elastic modulus E. As a consequence, it is harder to initiate failure in the case of hard slabs above a soft weak layer. This outcome is in agreement with the results of Camponovo and Schweizer (1997), Thumlert et al. (2013) and Thumlert and Jamieson (2014).

Our new skier propagation criterion was then applied to snow profiles observed in the field and compared to the RB score. The skier crack length obtained for a skier jumping and the critical crack length were correlated with the observed stability, i.e. the RB score, confirming the usefulness of the proposed approach to refine current stability estimates. However, a very high additional load $R = 3900$ N was necessary to obtain values of the skier crack length higher than zero. We argue that this is partly due to finite size effects of the Rutschblock

test. FEM simulations were performed with a relatively large system size (10 m) to prevent size effects. However, the Rutschblock has a side-length of 2 m with free side-wall boundary conditions which lead to higher stress concentrations in the weak layer. Hence, regarding this fact, the RB score underestimates stability. Still, the size of the Rutschblock is large enough to mimic both failure initiation and crack propagation, as reflected by the correlation between the RB score and the skier crack length as well as the critical crack length (Fig. 9). Future work should also try to correlate the quality of the failure (such as fracture character, van Herwijnen and Jamieson, 2007b) to the dynamics of crack propagation (Gaume et al., 2015a).

Furthermore, note that this new model is purely static and does not account for the dynamics of a moving skier which would have two opposite effects on avalanche release: i) its acceleration down the slope might lead to a decrease of the additional shear stress $\Delta\tau$ (except for sharp turns); ii) its track covering parts of the slope with varying snowpack properties would increase the likelihood to induce a crack in the weak layer. Our study also confirms one of the conclusions of Schweizer and Camponovo (2001), namely that a skier does not need to hit a (supposedly) pre-existing crack in a weak layer to trigger a slab avalanche. The skier crack length i.e. the zone over which the skier irreversibly damages the weak layer must be larger than the critical crack length to start the onset of crack propagation and possibly avalanche release.

Eventually, applying a framework as such, which couples failure initiation and crack propagation, will help in the future to obtain realistic distributions of snow instability over real terrain from measured or modeled snow cover data, such as recently tackled by Reuter et al. (2016b). Although our model accounts for both failure initiation and the onset of crack propagation, it needs to be completed by a criterion to assess the propensity of a tensile slab fracture – also in view of accounting for the potential size of avalanches. This step could be taken by comparing the slab tensile stress to the tensile strength (Schweizer et al., 2014; Reuter et al., 2016a; Gaume et al., 2015b; Benedetti et al., 2017). In particular, Reuter et al. (2016a) showed that accounting for a tensile criterion in addition to a failure initiation and crack propagation criteria significantly increased the accuracy of the instability classification.

5. Conclusions

We developed a new model to evaluate snow instability in skier triggered snow slab avalanches by combining failure initiation and crack propagation. At the depth of the weak layer, the model compares the skier crack length, i.e. the area over which the shear stress exceeds the shear strength, to the critical crack length for the onset of crack propagation. A sensitivity analysis allowed studying the effect of snowpack properties on the skier crack length and critical crack length. In particular, we showed that, even on flat terrain, failure initiation is more likely in shear than in compression. For realistic snowpack properties, it appeared that for weak layers buried deeper than approx. 0.6 m, failure initiation was rather unlikely, whereas crack propagation propensity remained high. A finite element analysis revealed that hard basal layers lead to relatively large stresses in the weak layer and large skier crack lengths thus promoting instability. In addition, for a constant load on the weak layer, stiff slabs led to lower stresses at the depth of the weak layer and lower skier crack lengths compared to soft slab layers. Finite element simulations were finally performed to compute the skier crack length and critical crack length for manually observed snow profiles, including slab layering and thus bridging effects. Combining the skier crack length and the critical crack length allowed to describe well the observed RB scores. The proposed approach can be useful to refine classical stability metrics by including crack propagation propensity and thus eventually improve avalanche forecasting and backcountry recreationist's safety.

Acknowledgments

We thank Jürg Schweizer and Alec van Herwijnen for fruitful discussion and comments on the paper. We also thank Bruce Jamieson and researchers of ASARC for the Rutschblock dataset. Johan Gaume has been supported by the Ambizione grant of the Swiss National Science Foundation (PZ00P2_161329).

References

Bazant, Z.P., Zi, G., McClung, D., 2003. Size effect law and fracture mechanics of the triggering of dry snow slab avalanches. J. Geophys. Res. 108 (B2), 2119.
Benedetti, L., Fischer, J.T., Gaume, J., 2017. A mechanically-based model of snow slab and weak layer fracture in the propagation saw test. Int. J. Solids Struct (In review).
Birkeland, K., van Herwijnen, A., Staples, M., Knoff, E., Bair, E., Simenhois, R., 2014. The role of slabs and weak layers in fracture arrest. In: In Proceedings International Snow Science Workshop 2014. Canada, Banff.
Camponovo, C., Schweizer, J., 1997. Measurements on skier triggering. In: Proceedings International Snow Science Workshop, Banff, Alberta, Canada, pp. 6–10.
Camponovo, C., Schweizer, J., 2001. Rheological measurements of the viscoelastic properties of snow. Ann. Glaciol. 32, 44–50.
Chandel, C., Mahajan, P., Srivastava, P., Kumar, V., 2014. The behaviour of snow under the effect of combined compressive and shear loading. Curr. Sci. 107, 888–894.
Fierz, C., Armstrong, R.L., Durand, Y., Etchevers, P., Greene, E., McClung, D.M., Nishimura, K., Satyawali, P.K., Sokratov, S.A., 2009. The International Classification for Seasonal Snow on the Ground. In: HP-VII Technical Documents in Hydrology, 83. France, UNESCO-IHP, Paris (90 pp.).
Föhn, P.M.B., 1987a. The Rutschblock as a practical tool for slope stability evaluation. In: Salm, B., Gubler, H. (Eds.), Symposium at Davos 1986 - Avalanche Formation, Movement and Effects. IAHS Publ., 162. International Association of Hydrological Sciences, Wallingford, Oxfordshire, U.K., pp. 223–228.
Föhn, P.M.B., 1987b. The stability index and various triggering mechanisms. In: Salm, B., Gubler, H. (Eds.), Symposium at Davos 1986–Avalanche Formation, Movement and Effects. IAHS Publ., 162. International Association of Hydrological Sciences, Wallingford, Oxfordshire, U.K., pp. 195–214.
Gaume, J., Chambon, G., Eckert, N., Naaim, M., 2013. Influence of weak-layer heterogeneity on snow slab avalanche release: application to the evaluation of avalanche release depths. J. Glaciol. 59 (215), 423–437.
Gaume, J., van Herwijnen, A., Chambon, G., Birkeland, K.W., Schweizer, J., 2015a. Modeling of crack propagation in weak snowpack layers using the discrete element method. Cryosphere 9, 1915–1932.
Gaume, J., Chambon, G., Eckert, N., Naaim, M., Schweizer, J., 2015b. Influence of weak layer heterogeneity and slab properties on slab tensile failure propensity and avalanche release area. Cryosphere 9, 795–804.
Gaume, J., van Herwijnen, A., Chambon, G., Wever, N., Schweizer, J., 2017. Snow fracture in relation to slab avalanche release: critical state for the onset of crack propagation. Cryosphere 11, 217–228.
Gauthier, D., Jamieson, B., 2008. Evaluation of a prototype field test for fracture and failure propagation propensity in weak snowpack layers. Cold Reg. Sci. Technol. 51 (2), 87–97.
Geldsetzer, T., Jamieson, J.B., 2001. Estimating Dry Snow Density From Grain Form and Hand Hardness, Proceedings International Snow Science Workshop, Big Sky, Montana, U.S.A., 1–6 October 2000. Montana State University, Bozeman MT, USA, pp. 121–127.
Habermann, M., Schweizer, J., Jamieson, J.B., 2008. Influence of snowpack layering on human-triggered snow slab avalanche release. Cold Reg. Sci. Technol. 54 (3), 176–182.
Heierli, J., Gumbsch, P., Zaiser, M., 2008. Anticrack nucleation as triggering mechanism for snow slab avalanches. Science 321 (5886), 240–243.
Heierli, J., Birkeland, K.W., Simenhois, R., Gumbsch, P., 2011. Anticrack model for skier triggering of slab avalanches. Cold Reg. Sci. Technol. 65 (3), 372–381.
van Herwijnen, A., Heierli, J., 2009. Measurement of crack-face friction in collapsed weak snow layers. Geophys. Res. Lett. 36 (23).
van Herwijnen, A., Jamieson, J.B., 2007a. Snowpack properties associated with fracture initiation and propagation resulting in skier-triggered dry snow slab avalanches. Cold Reg. Sci. Technol. 50 (1–3), 13–22.
van Herwijnen, A., Jamieson, B., 2007b. Fracture character in compression tests. Cold Reg. Sci. Technol. 47 (1), 60–68.
van Herwijnen, A., Gaume, J., Bair, E.H., Reuter, B., Birkeland, K.W., Schweizer, J., 2016. Estimating the effective elastic modulus and specific fracture energy of snowpack layers from field experiments. J. Glaciol. 62 (236), 997–1007.
Jamieson, J.B., Johnston, C.D., 1998. Refinements to the stability index for skier-triggered dry-slab avalanches. Ann. Glaciol. 26 (1), 296–302.
Jamieson, J.B., Johnston, C.D., 2001. Evaluation of the shear frame test for weak snowpack layers. Ann. Glaciol. 32, 59–68.
Jamieson, J.B., Schweizer, J., 2000. Texture and strength changes of buried surface-hoar layers with implications for dry snow-slab avalanche release. J. Glaciol. 46 (152), 151–160.
McClung, D.M., 2003. Size scaling for dry snow slab release. J. Geophys. Res. Solid Earth 108 (B10).
McClung, D.M., 2009. Dry snow slab quasi-brittle fracture initiation and verification from field tests. J. Geophys. Res. Earth Surf. 114, F01022.
Monti, F., Gaume, J., van Herwijnen, A., Schweizer, J., 2016. Snow instability evaluation:

calculating the skier-induced stress in a multi-layered snowpack. Nat. Hazards Earth Syst. Sci. 16 (3), 775–788.
Reiweger, I., Gaume, J., Schweizer, J., 2015. A new mixed-mode failure criterion for weak snowpack layers. Geophys. Res. Lett. 42, 1427–1432.
Reuter, B., Schweizer, J., van Herwijnen, A., 2015. A process-based approach to estimate point snow instability. Cryosphere 9, 837–847.
Reuter, B., van Herwijnen, A., Schweizer, J., 2016a. Observer independent measures of snow instability. In: Proceedings ISSW 2016. International Snow Science Workshop, Breckenridge, Colorado, USA.
Reuter, B., Richter, B., Schweizer, J., 2016b. Snow instability patterns at the scale of a small basin. J. Geophys. Res. Earth Surf. 121, 257–282, 2015JF003700.
Scapozza, C., 2004. Entwicklung eines dichte- und temperaturabhängigen Stoffgesetzes zur Beschreibung des visko-elastischen Verhaltens von Schnee. Ph.D. Thesis, ETH Zurich, Zurich, Switzerland. (250 pp.).
Schweizer, J., 1993. The influence of the layered character of snow cover on the triggering of slab avalanches. Ann. Glaciol. 18, 193–198.
Schweizer, J., Camponovo, C., 2001. The skier's zone of influence in triggering slab avalanches. Ann. Glaciol. 32, 314–320.
Schweizer, J., Jamieson, J.B., 2001. Snow cover properties for skier triggering of avalanches. Cold Reg. Sci. Technol. 33 (2–3), 207–221.
Schweizer, J., Jamieson, J.B., 2003. Snowpack properties for snow profile analysis. Cold Reg. Sci. Technol. 37 (3), 233–241.
Schweizer, J., Jamieson, J.B., Schneebeli, M., 2003. Snow avalanche formation. Rev. Geophys. 41 (4), 1016.
Schweizer, J., Reuter, B., van Herwijnen, A., Jamieson, J.B., Gauthier, D., 2014. On how the tensile strength of the slab affects crack propagation propensity. In: Haegeli, P. (Ed.), Proceedings ISSW 2014. International Snow Science Workshop, Banff, Alberta, Canada, 29 September – 3 October 2014, pp. 164–168.
Schweizer, J., Reuter, B., Van Herwijnen, A., Gaume, J., 2016a. Avalanche release 101. In: Proceedings ISSW 2016. International Snow Science Workshop, Breckenridge, Colorado, USA.
Schweizer, J., Reuter, B., van Herwijnen, A., Richter, B., Gaume, J., 2016b. Temporal evolution of crack propagation propensity in snow in relation to slab and weak layer properties. Cryosphere 10, 2637–2653.
Techel, F., Jarry, F., Kronthaler, G., Mitterer, S., Nairz, P., Pavšek, M., Valt, M., Darms, G., 2016. Avalanche fatalities in the European Alps: long-term trends and statistics. Geographica Helvetica 71 (2), 147–159.
Thumlert, S., Jamieson, B., 2014. Stress measurements in the snow cover below localized dynamic loads. Cold Reg. Sci. Technol. 106–107, 28–35.
Thumlert, S., Exner, T., Jamieson, B., Bellaire, S., 2013. Measurements of localized dynamic loading in a mountain snow cover. Cold Reg. Sci. Technol. 85 (0), 94–101.